Sodium chloride induced nitrogen salt with cyclo-N_5 anions at high pressure

Bi Zhang,[1] Meiling Xu,[1,2,*] Yu Xin,[2] Shuyi Lin,[3,1] Jian Hao,[1] Yanchao Wang,[2,†] and Yinwei Li[1,‡]

[1]*Laboratory of Quantum Functional Materials Design and Application, School of Physics and Electronic Engineering, Jiangsu Normal University, Xuzhou 221116, China*

[2]*Key Laboratory of Material Simulation Methods and Software of Ministry of Education and State Key Laboratory of Superhard Materials, College of Physics, Jilin University, Changchun 130012, China*

[3]*Department of Applied Physics, The Hong Kong Polytechnic University, Hunghom, Hong Kong 999077, China*

(Received 23 April 2024; accepted 6 August 2024; published 23 August 2024)

The energy landscape of sodium chloride-nitrogen mixtures has been comprehensively explored to examine the ability of the formation of unknown compounds under pressures of up to 100 GPa, using swarm-intelligence structure prediction methodology and first-principles calculations. We identified a thermodynamically stable NaN_5ClN_5 compound containing two cyclo-N_5 species under pressures exceeding 53 GPa, representing milder conditions in comparison to those requisite for pure solid nitrogen. In NaN_5ClN_5, the high electron affinity of the cyclo-N_5 motif allows it to oxidize the chlorine atoms, resulting in the formation of two cyclo-N_5 anions. Additionally, the weak covalent interactions between Cl and nearby N atoms plays a key role in stabilization of structure. It has been demonstrated that simple NaN_5 salt was a suitable precursor for the synthesis of NaN_5ClN_5 at high pressure. *Ab initio* molecular dynamics simulations demonstrated the recoverability of NaN_5ClN_5 as a metastable phase at ambient pressure-temperature conditions. Additionally, NaN_5ClN_5 exhibits a higher energy density of 3.86 kJ/g and a lower mass density of 1.67 g/cm^3 in comparison to metal pentazolate salts, highlighting its potential as a high energy-density material.

DOI: 10.1103/PhysRevResearch.6.033213

I. INTRODUCTION

Polynitrogens have garnered significant attention in condensed matter physics and materials science as they are considered promising for the development of environmentally friendly high energy-density materials (HEDMs) [1–3]. The successful preparation of polynitrogen in the experiment is encouraging despite the need for more than a million atmospheres of pressure [4–7]. However, the practical application of pure polynitrogen as HEDMs presents challenges due to its inherent instability under atmospheric conditions [8–25].

The approach to address the challenges associated with pure polynitrogen is the incorporation of additional elements, which can effectively lower the required pressure for nitrogen polymerization, a phenomenon referred to as "chemical precompression" effects [26–28]. Numerous nitrogen-rich compounds have been investigated in experiments and theory, such as MN_5 (M = Li, Na, K, Rb, Cs, Cu, etc.) [29–36], MN_6 (M = Ba, W, Sn, Gd, etc.) [37–40], MN_{10} (M = Be, Mg, Ba, Zn, etc.) [41,42], and MN_{15} (M = Al, Ca, Sc, Y, etc.) [43]. Theoretical studies have suggested that these compounds usually exhibit thermodynamical stability at pressures below 100 GPa and have the potential for recovery under ambient conditions [44–52]. Of particular note is the potential retrieval of LiN_5 at ambient conditions [30], suggesting the possibility of utilizing alkali-metal pentazolate salts as HEDMs.

Ionic compounds can capture nitrogen molecules, and even induce the formation of a polymeric nitrogen network under high-pressure conditions [53]. Our work has demonstrated that alkali metal fluorides can act as catalysts for the decomposition of nitrogen molecules for the formation of MN_5N_5F (M = Li, Na, and K) compounds under high-pressure conditions [54]. This catalytic activity allows for the creation of the elusive cyclo-N_5^+ cation and the assembly of the long-sought $N_5^+N_5^-$ salt, indicating the ability of ionic compounds to induce the formation of a polymeric nitrogen network. The ability to create polymeric nitrogen networks through tailored ionic compounds opens up new possibilities for the synthesis and stabilization of nitrogen-rich materials with desirable properties.

In this work, we selected NaCl as a catalyst to investigate its potential for storing nitrogen molecules and catalyzing the formation of a polymeric nitrogen network under high-pressure conditions. Of particular interest is that we identified a thermodynamically stable NaN_5ClN_5 compound under pressures exceeding 53 GPa, and N atoms polymerize into two cyclo-N_5 species in this compound. Bader analysis and Mulliken population analysis revealed that two cyclo-N_5 species are ionic due to a stronger oxidizing power of cyclo-N_5 than that of the Cl atom. Additionally, there exists the weak covalent interactions between Cl and nearest neighbor N atoms. Phonon spectra calculations and *ab initio* molecular dynamics

*Contact author: xml@calypso.cn
†Contact author: wyc@calypso.cn
‡Contact author: yinwei_li@jsnu.edu.cn

(AIMD) simulations suggest that NaN_5ClN_5 has the potential to maintain its cyclo-N_5 framework under atmospheric conditions, highlighting its promise as HEDMs.

II. COMPUTATION METHODS

Structure prediction simulations for $NaClN_x$ (x = 1–10) compounds with 1–4 formula units were performed using the CALYPSO method [55–59] at pressures of 30, 50, and 100 GPa. Structure relaxations and electronic property calculations were performed within the framework of density functional theory [60] using the Perdew-Burke-Ernzerhof generalized gradient approximation [61], as implemented in the Vienna *ab initio* simulation package [62]. The electron-ion interactions are considered by the projector-augmented-wave potentials [63], with s^1, s^2p^5, and s^2p^3 configurations as valence electrons for Na, Cl, and N atoms, respectively. A plane-wave cutoff energy of 600 eV was employed, along with Monkhorst-Pack k-point meshes [64] with a grid spacing of $2\pi \times 0.03$ Å^{-1}. These settings were chosen to ensure energy and force convergence with precisions of 10^{-6} eV and 0.01 eV Å^{-1}, respectively. Phonon spectra calculations were carried out using the direct supercell ($2\times1\times1$) methods implemented in the PHONOPY code [65]. AIMD simulations are performed using the Nosé-Hoover chain thermostat for 10 ps with a time step of 1 fs at 300 K. The simulation supercell had dimensions of $2\times1\times1$, containing a total of 96 atoms. The temperature-dependent effective potential method was used to determine the influence of thermal effects on the phonon dispersion relations [66–68]. This method is based on AIMD and accounts for anharmonic phonon-phonon interactions occurring at finite temperatures. It does so by constructing interatomic force-constant matrices using information obtained from AIMD trajectories.

III. RESULTS AND DISCUSSION

Figure 1(a) presents the convex hull diagram at selected pressures based on the formation enthalpy calculations of $NaClN_x$ compounds. At ambient pressure, our calculations indicate the absence of any thermodynamically stable $NaClN_x$ compounds, as they exhibit positive enthalpies in comparison to sodium chloride and α-N. At a pressure of 50 GPa, three compounds, namely $(NaCl)_2N_2$, $NaClN_2$, and $NaCl(N_2)_4$, are predicted to be stable, forming the vertices of the convex hull. At a pressure of 100 GPa, only NaN_5ClN_5 becomes the only thermodynamically stable phase. Figure 1(b) illustrates the pressure-composition phase diagram of these thermodynamically stable structures. At pressure as low as 18 GPa, P-1 $(NaCl)_2N_2$ becomes stable, and at 26 GPa, $P1$ $NaCl(N_2)_4$ stabilizes; both remain stable until 58 GPa. $Cmcm$ $NaClN_2$ exhibits stability at 44 GPa and transforms into $P63/mmc$ $NaClN_2$ at 51.5 GPa. $(NaCl)_2N_2$, $NaClN_2$, and $NaCl(N_2)_4$ are hybrid compounds, in which nitrogen is stored within the crystal lattice in the form of nitrogen molecules (Fig. S1 and Table S1 in the Supplemental Material (SM) [69]). Electronic properties calculations show that these hybrid compounds are semiconductors with band gaps of 0.92–3.25 eV. The valence band maximum and conduction band minimum are mainly

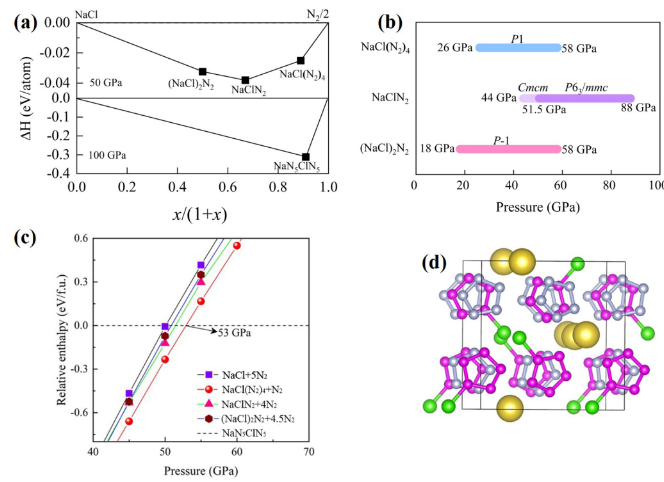

FIG. 1. (a) Convex hull of formation enthalpies (ΔH) of NaCl - N system with respect to decomposition into solid NaCl and N_2 at selected pressures, defined as ΔH = [H($NaClN_x$) - H(NaCl) - xH(N)]/1 + x. (b) Pressure-composition phase diagrams of the predicted NaCl–N_x compounds at 0–100 GPa. The stable phases of solid nitrogen and sodium chloride at varying pressures were selected as reference structures. Nitrogen adopts α-N (0–9.5 GPa) and ϵ-N (9.5–100 GPa) phases [16], while sodium chloride adopts the fcc (0–30 GPa) and $Pm3m$ (30–100 GPa) structures [70]. (c) Formation enthalpy of $P2_12_12_1$ NaN_5ClN_5 with respect to different decomposition paths as a function of pressure. (d) Crystal structure of NaN_5ClN_5. Yellow and green spheres represent Na and Cl atoms, respectively. N atoms in two N_5 rings are shown in gray and pink spheres, respectively.

contributed by the Cl p and N p states, respectively (Fig. S2 within the SM [69]). Phonon spectra calculations indicate their dynamical stability at high pressure (Fig. S3 within the SM [69]). The formation enthalpy of NaN_5ClN_5 in relation to its decomposition pathways into NaCl + $5N_2$, $NaCl(N_2)_4$ + N_2, $NaClN_2 + 4N_2$, and $(NaCl)_2N_2 + 4.5N_2$ has been provided in Fig. 1(c). Results demonstrated that NaN_5ClN_5 becomes stable beyond 53 GPa and persists until the highest pressure (100 GPa) considered in our study. NaN_5ClN_5 crystallizes in an orthogonal structure with space group $P2_12_12_1$. N atoms polymerize into two types of N_5 rings which are distinguished by different (pink and gray) colored atoms [Fig. 1(d)]. This structural arrangement is reminiscent of the XN_5N_5F (X = Li, Na, and K) structure reported in our previous work. The average N-N bond length within the cyclo-N_5 rings is ∼1.28 Å, falling between a single bond and a double bond. The Cl atoms preferentially bond to one type of N_5 ring with the N-Cl bond length of 1.65 Å. Electronic properties calculations for NaN_5ClN_5 reveal the semiconductive nature with a band gap of 1.82 eV (Fig. S2 within the SM [69]).

It was demonstrated that in NaN_5N_5F, the cyclo-N_5 moiety transfers the electron to the F atom, driven by the higher oxidizing ability of F in comparison to cyclo-N_5, leading to the formation of a cyclo-N_5^+ cation and the assembly of $N_5^+N_5^-$ salt in a NaF compound [54]. Consequently, a natural question arises: how is the oxidizing ability of the cyclo-N_5 moiety in comparison with Cl and Br atoms at high pressure?

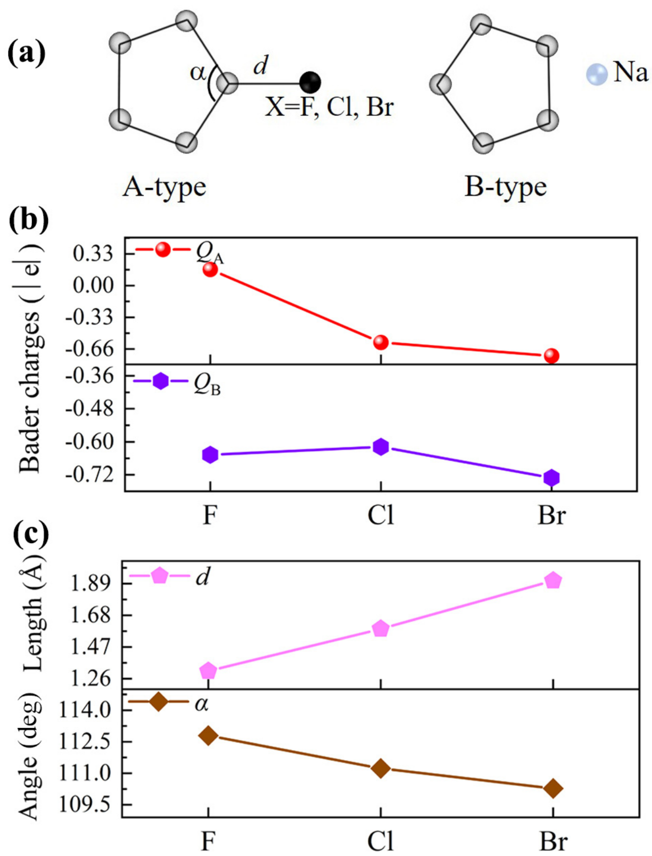

FIG. 2. (a) N_5F, ClN_5, BrN_5, and NaN_5 units in corresponding compounds. (b) Bader charges of A-type and B-type cyclo-N_5 for NaN_5N_5F and NaN_5XN_5 (X = Cl and Br). (c) The average lengths of N-N bonds in A-type cyclo-N_5 for NaN_5N_5F, NaN_5ClN_5, and NaN_5BrN_5 at 100 GPa.

NaN_5BrN_5 structure was first constructed by substituting Cl with Br in NaN_5ClN_5. After performing a full optimization, it was observed that NaN_5BrN_5 possesses a higher symmetry compared to NaN_5ClN_5. Specifically, the space group of NaN_5BrN_5 was determined to be P-42_1m. The two N_5 rings were found to be equivalent and Br atoms do not show a preference for one of the N_5 rings (Fig. S4 within the SM [69]).

Figure 2(a) depicts the two types of cyclo-N_5 rings in NaN_5N_5F, NaN_5ClN_5, and NaN_5BrN_5 which are designated as A-type and B-type cyclo-N_5. Bader charge analysis, based on the partition of charge density, was used to determine charge transfer between cyclo-N_5 and halogen elements, as depicted in Fig. 2(b) and Table S2 within the SM [69]. It was demonstrated that A-type cyclo-N_5 in NaN_5N_5F transfers 0.168 |e| to the F atom due to the stronger oxidizing power of F compared to cyclo-N_5. As a contrast, A-type cyclo-N_5 species in NaN_5XN_5 (X = Cl and Br) gain 0.592 and 0.731 |e| from Cl and Br atoms, respectively, indicating that cyclo-N_5 exhibits stronger oxidizing power than Cl and Br. Therefore, the two N_5 rings in NaN_5XN_5 (X = Cl and Br) are cyclo-N_5^- anions.

The ability of the cyclo-N_5 species to gain or lose electrons compared to halogen elements can influence the bond length between N and the halogen element. As indicated in Fig. 2(c) and Table S3 within the SM [69], the N-halogen bond length exhibits a gradual increase as the electronegativity of the halogen element decreases. Specifically, the N-halogen bond lengths in NaN_5N_5F, NaN_5ClN_5, and NaN_5ClN_5 are 1.31, 1.59, and 1.91 Å, respectively. Correspondingly, the angles of $\angle$ N1-N2-N3 (α) in A-type cyclo-N_5 are gradually decreased from 112.79° (NaN_5N_5F) to 110.28° (NaN_5BrN_5).

Mulliken population analysis derived directly from the overlap of atomic orbitals [71] was used to further examine the electron-accepting/donating ability of Cl and N atoms in compounds. As tabulated in Table I, the calculated results are consistent with those from the Bader analysis. In NaN_5ClN_5, Cl loses 0.45 |e| to the nearby cyclo-N_5 group, forming cyclo-N_5^- ions. Based on Mulliken population analysis, we noted weak covalent interactions between N and Cl atoms and the ionic interactions between N and Br atoms. The electron population in N-Cl bonds is 0.19, which is significantly smaller than the electron population (0.90–0.94) in the N-N bonds. This indicates that the N-Cl interactions have a relatively weak covalent character compared to the stronger N-N bonds. Additionally, the electron localization function (ELF) calculations, as shown in Fig. 3, further support the conclusion of weak covalent N-Cl interactions and ionic interactions between N and Br atoms. ELF also exhibit a polarized covalent N-Cl bond, which is biased toward the N atoms. Furthermore, the electron density difference calculations (Fig. 4) show that the Cl and Br atoms indeed transfer electrons to the nearest neighbor N atoms. Therefore, two cyclo-N_5 units are anions in NaN_5N_5F and NaN_5BrN_5.

The presence of a common cyclo-N_5 motif in simple metal salts suggests that the NaN_5 salt provides a suitable starting material for the synthesis of NaN_5XN_5 (X = Cl and Br) compounds. We calculated the formation enthalpy of NaN_5XN_5

TABLE I. Mulliken population analysis for NaN_5ClN_5 and NaN_5BrN_5 at 100 GPa.

Compounds	Species	s orbit (e)	p orbit (e)	Charge (e)	Bond	Length (Å)	Population
NaN_5ClN_5	Na	1.95	5.59	1.36	N-N	1.27–1.29	0.86–0.96
	Cl	1.95	4.59	0.45	N-Cl	1.59	0.19
	cyclo-N_5	7.73	18.16	−0.89	Na-N	1.99	−0.38
	cyclo-N_5	7.84	18.07	−0.92			
NaN_5BrN_5	Na	1.92	5.99	1.09	N-N	1.27-1.30	0.79–0.90
	Br	1.65	4.40	0.95	N-Br	1.90	−0.41
	cyclo-N_5	7.87	36.1	−0.94	Na-N	2.04	−0.20
	cyclo-N_5	7.83	18.26	−1.10			

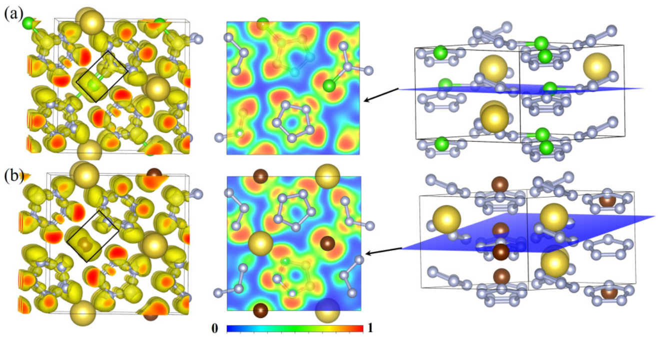

FIG. 3. Three-dimensional (isovalue = 0.75) and two-dimensional ELF maps of (a) NaN_5ClN_5 and (b) NaN_5BrN_5 at 100 GPa.

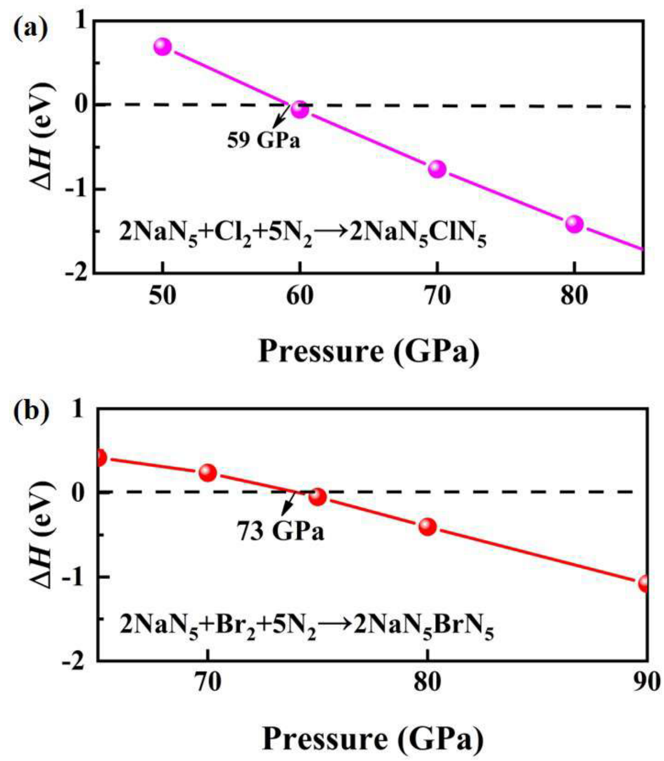

FIG. 5. Calculated enthalpy as a function of pressure of NaN_5XN_5 (X = Cl and Br) compounds relative to the experimentally found NaN_5. Negative relative enthalpy indicates the stability of the NaN_5XN_5 compounds. We adopted *Cmca* Cl, *Cmca* Br (65–80 GPa), and *Immm* Br (81–90 GPa) as decomposition products.

with respect to NaN_5, ϵ-N, and X elements as a function of pressure. Figure 5 illustrates that NaN_5ClN_5 and NaN_5BrN_5 become energetically stable at pressures of 59 and 73 GPa, respectively, lower than the pressure required to synthesize cg-N.

The absence of imaginary frequencies throughout the entire Brillouin zone in the phonon dispersion curve indicates the dynamical stability of NaN_5XN_5 (X = Cl and Br) under high pressure [Figs. 6(a) and 6(b)]. Based on AIMD simulations at 300 K, it has been observed that the energy oscillation of NaN_5ClN_5 and NaN_5BrN_5 compounds remains within a small energy range of 10.5 meV/atom at 55 GPa and 11.9 meV/atom at 75 GPa, respectively [Figs. 6(c) and 6(d)]. Furthermore, a comparison between the initial and final structures of NaN_5ClN_5 and NaN_5BrN_5 reveals that the cyclo-N_5 motif and overall crystal structure are well preserved. This suggests that the NaN_5XN_5 compounds maintain their structural integrity without significant changes under the examined temperature and pressure conditions. Phonon spectra calculations were further conducted to assess the dynamical stability of NaN_5XN_5 at ambient pressure. As shown in Fig. 7(a), the absence of unstable vibration modes in the full Brillouin zone confirmed the dynamical stability of NaN_5ClN_5. For NaN_5BrN_5, the negative frequencies are presented in the phonon relation curves, suggesting dynamical instability [Fig. 7(b)].

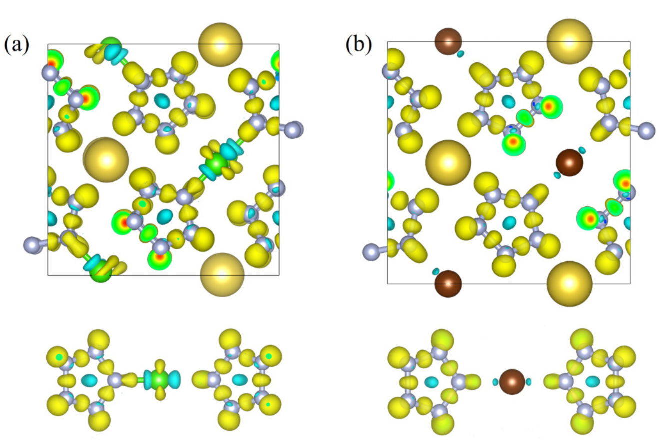

FIG. 4. Electron density difference (isovalue = 0.028 e/bohr^3) for (a) NaN_5ClN_5 and (b) NaN_5BrN_5 at 100 GPa. The yellow and blue regions represent electron accumulation and deflection, respectively.

To provide a more accurate assessment of the recoverability of NaN_5XN_5 under atmospheric conditions, kinetic stability which indicates a resilience against structural changes was evaluated through AIMD simulations performed at 300 K. AIMD simulations take into account the thermal motion of atoms and provide insight into the materials' behavior under realistic conditions. Figures 7(c) and 7(d) present the energy oscillation profiles of NaN_5XN_5 compounds. For NaN_5ClN_5 at ambient pressure, the energy oscillation is comparable to that observed in the high-pressure state. This indicates that there are no significant changes in the structural stability of NaN_5ClN_5 during the 10-ps simulation runs. The final state structure closely resembles the initial structure, suggesting that NaN_5ClN_5 maintains its structural integrity. In the case of NaN_5BrN_5, a slight increase of ~18 meV/atom in energy oscillation is observed compared to the high-pressure state. However, this increase remains within an acceptable range. The cyclo-N_5 species in NaN_5BrN_5 retain their structural integrity and largely remain in their original crystal positions. The results from the AIMD simulations confirm the thermal stability and recoverability of NaN_5XN_5 compounds under ambient pressure-temperature conditions. Therefore, upon synthesis at high pressure, NaN_5XN_5 is likely to be recoverable as a metastable phase once the pressure is released.

Given the inherent recoverability of NaN_5XN_5 (X = Cl and Br) as a metastable phase in environmental conditions,

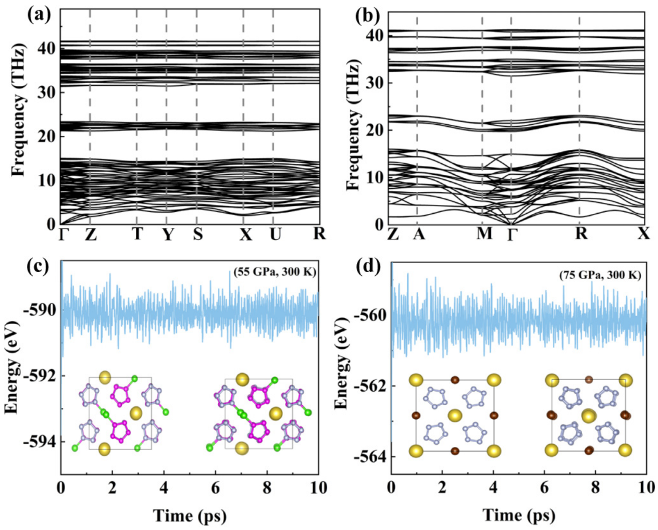

FIG. 6. Phonon dispersion curves of (a) $P2_12_12_1$ NaN_5ClN_5 at 55 GPa and (b) P-42_1m NaN_5BrN_5 at 75 GPa (300 K). Evolution of energies during the AIMD simulations at 300 K of (c) $P2_12_12_1$ NaN_5ClN_5 at 55 GPa and (d) P-42_1m NaN_5BrN_5 at 75 GPa.

we conducted further assessments to evaluate its potential as a HEMD. Total energy calculations were performed to compare NaN_5XN_5 compounds with NaX ionic compounds and α-N_2. The results indicate that the energy density of NaN_5ClN_5 is estimated to be 3.86 kJ/g, slightly larger than that (3.77 kJ/g) of NaN_5BrN_5. In addition, NaN_5ClN_5 possesses a smaller mass density of 1.67 g/cm^3 than that (2.78 g/cm^3) of NaN_5BrN_5. Figure 8 provides a comparison of energy density versus mass density for NaN_5XN_5 compounds with well-known HEDMs and metal nitrides containing N_5 molecules. It is noted that NaN_5ClN_5 exhibits comparable energy density (3.86 kJ/g) and mass density

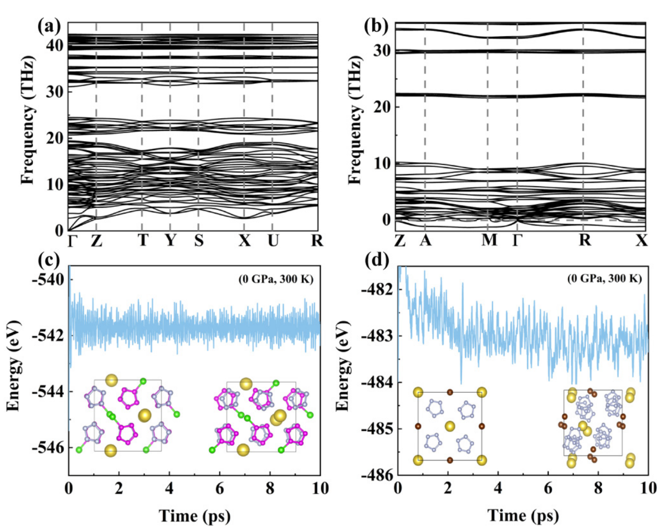

FIG. 7. Phonon dispersion curves of (a) $P2_12_12_1$ NaN_5ClN_5 and (b) P-42_1m NaN_5BrN_5 at 0 GPa. Evolution of energies during the ambient-pressure AIMD simulations at 300 K of (c) $P2_12_12_1$ NaN_5ClN_5 and (d) P-42_1m NaN_5BrN_5.

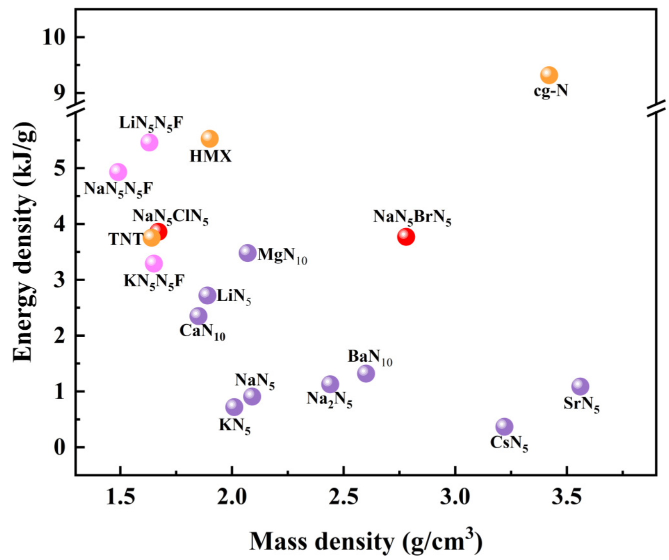

FIG. 8. Energy density versus mass density for NaN_5XN_5 (X = Cl and Br), compared to various metal nitrides with N_5 ring, cg-N, and the well-established HEDMs.

(1.67 g/cm3) to TNT (3.76 kJ/g and 1.64 g/cm3) [72], also possessing higher energy density and lower mass density than metal nitrides. Although the energy density of NaN_5ClN_5 is lower than that of cg-N (9.7 kJ/g) [51], its mass density is only half of cg-N (3.42 g/cm^3). Our findings highlight the potential of NaN_5ClN_5 as a HEMD, attributed to the balanced combination of elevated energy release and reduced mass density.

IV. CONCLUSION

In summary, using the CALYPSO method in conjunction with first-principles calculations, we comprehensively explored the high-pressure phase diagram of sodium chloride-nitrogen mixtures. Three thermodynamically stable hybrid compounds, including $(NaCl)_2N_2$, $NaCl(N_2)_4$, and $NaClN_2$ have been identified at low pressure. We also identified a NaN_5ClN_5 compound with polymeric nitrogen which is thermodynamically stable at pressures above 53 GPa. The bond characteristics analysis reveals that the cyclo-N_5 motif has a stronger electron-accepting ability compared to the Cl atom, leading to the formation of two cyclo-N_5 anions. The same conclusion can be drawn from the analysis of the NaN_5BrN_5 compound, where a similar charge transfer and anion formation process occurs. Furthermore, the analysis indicates the presence of weak, polar covalent interactions between the Cl atoms and the neighboring cyclo-N_5 units, play a critical role in structure stability. It has been demonstrated that NaN_5 salts containing the cyclo-N_5 motif can serve as suitable starting materials for the synthesis of NaN_5ClN_5 under high pressures exceeding 59 GPa. AIMD simulations suggested the stability and recoverability of NaN_5ClN_5 as a metastable phase under atmosphere conditions. The combination of a higher energy density and lower mass density in NaN_5ClN_5 makes it a promising candidate for HEDM applications. These findings highlight the potential of NaN_5ClN_5 and the comprehensive exploration of sodium chloride-nitrogen mixtures in advancing the understanding of high-pressure chemistry and the development of materials with desirable properties.

ACKNOWLEDGMENTS

The authors acknowledge funding support from the National Key Research and Development Program of China (Grant No. 2022YFA1402304), the National Natural Science Foundation of China (Grants No. T2225013, No. 12374010, No. 12174142, No. 12074154, and No. 11904142), the Six Talent Peaks Project, the 333 High-level Talents Project of Jiangsu Province, and the Open Project of State Key Laboratory of Superhard Materials, Jilin University (Grant No. 202417). Computational resources were provided by the High-performance Computing Center of the School of Physics and Electronic Engineering of Jiangsu Normal University and the High-Performance Computing Center of Jilin University.

[1] M. Miao, Y. Sun, E. Zurek, and H. Lin, Chemistry under high pressure, Nat. Rev. Chem. **4**, 508 (2020).

[2] L. Zhang, Y. Wang, J. Lv, and Y. Ma, Materials discovery at high pressures, Nat. Rev. Mater. **2**, 17005 (2017).

[3] M. Xu, Y. Li, and Y. Ma, Materials by design at high pressures, Chem. Sci. **13**, 329 (2022).

[4] M. I. Eremets, A. G. Gavriliuk, I. A. Trojan, D. A. Dzivenko, and R. Boehler, Single-bonded cubic form of nitrogen, Nat. Mater. **3**, 558 (2004).

[5] D. Tomasino, M. Kim, J. Smith, and C.-S. Yoo, Pressure-induced symmetry-lowering transition in dense nitrogen to layered polymeric nitrogen (LP-N) with colossal Raman intensity, Phys. Rev. Lett. **113**, 205502 (2014).

[6] D. Laniel, G. Geneste, G. Weck, M. Mezouar, and P. Loubeyre, Hexagonal layered polymeric nitrogen phase synthesized near 250 GPa, Phys. Rev. Lett. **122**, 066001 (2019).

[7] D. Laniel, B. Winkler, T. Fedotenko, A. Pakhomova, S. Chariton, V. Milman, V. Prakapenka, L. Dubrovinsky, and N. Dubrovinskaia, High-pressure polymeric nitrogen allotrope with the black phosphorus structure, Phys. Rev. Lett. **124**, 216001 (2020).

[8] M. J. Greschner, M. Zhang, A. Majumdar, H. Liu, F. Peng, J. S. Tse, and Y. Yao, A new allotrope of nitrogen as high-energy density material, J. Phys. Chem. A **120**, 2920 (2016).

[9] B. Hirshberg, R. B. Gerber, and A. I. Krylov, Calculations predict a stable molecular crystal of N_8, Nat. Chem. **6**, 52 (2014).

[10] X. Wang, Y. Wang, M. Miao, X. Zhong, J. Lv, T. Cui, J. Li, L. Chen, C. J. Pickard, and Y. Ma, Cagelike diamondoid nitrogen at high pressures, Phys. Rev. Lett. **109**, 175502 (2012).

[11] S. Liu, L. Zhao, M. Yao, M. Miao, and B. Liu, Novel all-nitrogen molecular crystals of aromatic N_{10}, Adv. Sci. **7**, 1902320 (2020).

[12] S. Lin, M. Xu, Y. Liang, X. Yuan, Y. Zhang, F. Wang, J. Hao, and Y. Li, Ambient-pressure recoverable polynitrogen solids assembled by pentazolate rings with high energy density, Inorg. Chem. **61**, 15532 (2022).

[13] L. Zhao, S. Liu, Y. Chen, W. Yi, D. Khodagholian, F. Gu, E. Kelson, Y. Zheng, B. Liu, and M. Miao, A novel all-nitrogen molecular crystal N_{16} as a promising high-energy-density material, Dalton Trans. **51**, 9369 (2022).

[14] X. Wang, F. Tian, L. Wang, T. Cui, B. Liu, and G. Zou, Structural stability of polymeric nitrogen: A first-principles investigation, J. Chem. Phys. **132**, 024502 (2010).

[15] Y. Yao, J. S. Tse, and K. Tanaka, Metastable high-pressure single-bonded phases of nitrogen predicted via genetic algorithm, Phys. Rev. B **77**, 052103 (2008).

[16] C. J. Pickard and R. J. Needs, High-pressure phases of nitrogen, Phys. Rev. Lett. **102**, 125702 (2009).

[17] F. Zahariev, J. Hooper, S. Alavi, F. Zhang, and T. K. Woo, Low-pressure metastable phase of single-bonded polymeric nitrogen from a helical structure motif and first-principles calculations, Phys. Rev. B **75**, 140101 (2007).

[18] M. Sun, Y. Yin, and Z. Pang, Predicted new structures of polymeric nitrogen under 100-600 GPa, Comput. Mater. Sci. **98**, 399 (2015).

[19] S. V. Bondarchuk and B. F. Minaev, Two-dimensional honeycomb (A7) and zigzag sheet (ZS) type nitrogen monolayers. a first principles study of structural, electronic, spectral, and mechanical properties, Comput. Mater. Sci. **133**, 122 (2017).

[20] J. Kotakoski and K. Albe, First-principles calculations on solid nitrogen: A comparative study of high-pressure phases, Phys. Rev. B **77**, 144109 (2008).

[21] Y. Ma, A. R. Oganov, Z. Li, Y. Xie, and J. Kotakoski, Novel high pressure structures of polymeric nitrogen, Phys. Rev. Lett. **102**, 065501 (2009).

[22] X. Wang, Z. He, Y. Ma, T. Cui, Z. Liu, B. Liu, J. Li, and G. Zou, Prediction of a new layered phase of nitrogen from first-principles simulations, J. Phys.: Condens. Matter **19**, 425226 (2007).

[23] W. D. Mattson, D. Sanchez-Portal, S. Chiesa, and R. M. Martin, Prediction of new phases of nitrogen at high pressure from first-principles simulations, Phys. Rev. Lett. **93**, 125501 (2004).

[24] X. Wang, F. Tian, L. Wang, X. Jin, D. Duan, X. Huang, B. Liu, and T. Cui, Predicted novel metallic metastable phases of polymeric nitrogen at high pressures, New J. Phys. **15**, 013010 (2013).

[25] F. Zahariev, A. Hu, J. Hooper, F. Zhang, and T. Woo, Layered single-bonded nonmolecular phase of nitrogen from first-principles simulation, Phys. Rev. B **72**, 214108 (2005).

[26] W. Yi, L. Zhao, X. Liu, X. Chen, Y. Zheng, and M. Miao, Packing high-energy together: Binding the power of pentazolate and high-valence metals with strong bonds, Mater. Des. **193**, 108820 (2020).

[27] J. Yuan, K. Xia, C. Ding, X. Wang, Q. Lu, and J. Sun, High-energy-density metal nitrides with armchair chains, Matter Radiat. Extremes **7**, 038402 (2022).

[28] J. Zhang, A. R. Oganov, X. Li, and H. Niu, Pressure-stabilized hafnium nitrides and their properties, Phys. Rev. B **95**, 020103(R) (2017).

[29] F. Peng, Y. Yao, H. Liu, and Y. Ma, Crystalline LiN_5 predicted from first-principles as a possible high-energy material, J. Phys. Chem. Lett. **6**, 2363 (2015).

[30] D. Laniel, G. Weck, G. Gaiffe, G. Garbarino, and P. Loubeyre, High-pressure synthesized lithium pentazolate compound metastable under ambient conditions, J. Phys. Chem. Lett. **9**, 1600 (2018).

[31] B. A. Steele and I. I. Oleynik, Sodium pentazolate: A nitrogen rich high energy density material, Chem. Phys. Lett. **643**, 21 (2016).

[32] B. A. Steele and I. I. Oleynik, Novel potassium polynitrides at high pressures, J. Phys. Chem. A **121**, 8955 (2017).

[33] A. S. Williams, B. A. Steele, and I. I. Oleynik, Novel rubidium poly-nitrogen materials at high pressure, J. Chem. Phys. **147**, 234701 (2017).

[34] B. A. Steele, E. Stavrou, J. C. Crowhurst, J. M. Zaug, V. B. Prakapenka, and I. I. Oleynik, High-pressure synthesis of a pentazolate salt, Chem. Mater. **29**, 735 (2017).

[35] F. Peng, Y. Han, H. Liu, and Y. Yao, Exotic stable cesium polynitrides at high pressure, Sci. Rep. **5**, 16902 (2015).

[36] J. Li, L. Sun, X. Wang, H. Zhu, and M. Miao, Simple route to metal cyclo-N_5^- salt: High-pressure synthesis of CuN_5, J. Phys. Chem. C **122**, 22339 (2018).

[37] N. P. Salke, K. Xia, S. Fu, Y. Zhang, E. Greenberg, V. B. Prakapenka, J. Liu, J. Sun, and J.-F. Lin, Tungsten hexanitride with single-bonded armchairlike hexazine structure at high pressure, Phys. Rev. Lett. **126**, 065702 (2021).

[38] L. Liu, D. Wang, S. Zhang, and H. Zhang, Pressure-stabilized GdN_6 with an armchair–antiarmchair structure as a high energy density material, J. Mater. Chem. A **9**, 16751 (2021).

[39] B. Huang and G. Frapper, Barium–nitrogen phases under pressure: Emergence of structural diversity and nitrogen-rich compounds, Chem. Mater. **30**, 7623 (2018).

[40] B. Wang, R. Larhlimi, H. Valencia, F. Guégan, and G. Frapper, Prediction of novel tin nitride Sn_xN_y phases under pressure, J. Phys. Chem. C **124**, 8080 (2020).

[41] J. Yuan, K. Xia, J. Wu, and J. Sun, High-energy-density pentazolate salts: CaN_{10} and BaN_{10}, Sci. China Phys. Mech. Astron. **64**, 218211 (2021).

[42] Z. Liu, D. Li, F. Tian, D. Duan, H. Li, and T. Cui, Moderate pressure stabilized pentazolate cyclo-N_5^- anion in $Zn(N_5)_2$ salt, Inorg. Chem. **59**, 8002 (2020).

[43] K. Xia, J. Yuan, X. Zheng, C. Liu, H. Gao, Q. Wu, and J. Sun, Predictions on high-power trivalent metal pentazolate salts, J. Phys. Chem. Lett. **10**, 6166 (2019).

[44] Y. Wang, Z. Li, R. Li, Y. Li, S. Liu, Z. Yao, and B. Liu, Two ultrahigh-energy-density layered cerium polynitrides with molecular sieve cchannel, Inorg. Chem. **62**, 11674 (2023).

[45] Z. Raza, C. J. Pickard, C. Pinilla, and A. M. Saitta, High energy density mixed polymeric phase from carbon monoxide and nitrogen, Phys. Rev. Lett. **111**, 235501 (2013).

[46] J. Zhang, C. Niu, H. Zhang, J. Zhao, X. Wang, and Z. Zeng, Polymerization of nitrogen in nitrogen-fluorine compounds under pressure, J. Phys. Chem. Lett. **12**, 5731 (2021).

[47] S. Niu, D. Xu, H. Li, Z. Yao, S. Liu, C. Zhai, K. Hu, X. Shi, P. Wang, and B. Liu, Pressure-stabilized polymerization of nitrogen in manganese nitrides at ambient and high pressures, Phys. Chem. Chem. Phys. **24**, 5738 (2022).

[48] D. Laniel, B. Winkler, E. Koemets, T. Fedotenko, M. Bykov, E. Bykova, L. Dubrovinsky, and N. Dubrovinskaia, Synthesis of magnesium-nitrogen salts of polynitrogen anions, Nat. Commun. **10**, 4515 (2019).

[49] Y. Liu, R. Wang, Z. Wang, D. Li, and T. Cui, Formation of twelve-fold iodine coordination at high pressure, Nat. Commun. **13**, 412 (2022).

[50] F. Peng, Y. Ma, A. Hermann, and M. Miao, Recoverable high-energy compounds by reacting methane and nitrogen under high pressure, Phys. Rev. Mater. **4**, 103610 (2020).

[51] Y. Li, X. Feng, H. Liu, J. Hao, S. A. Redfern, W. Lei, D. Liu, and Y. Ma, Route to high-energy density polymeric nitrogen *t*-N via He-N compounds, Nat. Commun. **9**, 722 (2018).

[52] F. Peng, Y. Wang, H. Wang, Y. Zhang, and Y. Ma, Stable xenon nitride at high pressures, Phys. Rev. B **92**, 094104 (2015).

[53] F. Peng, Y. Ma, C. J. Pickard, H. Liu, and M. Miao, Universal insertion of molecules in ionic compounds under pressure, Natl. Sci. Rev. **11**, nwae016 (2024).

[54] B. Zhang, Y. Xin, M. Xu, Y. Zhang, Y. Li, Y. Wang, and C. Chen, Creating cyclo-N_5^+ cation and assembling $N_5^+N_5^-$ salt via electronegativity co-matching in tailored ionic compounds, arXiv:2405.06262.

[55] Y. Wang, J. Lv, L. Zhu, and Y. Ma, Crystal structure prediction via particle-swarm optimization, Phys. Rev. B **82**, 094116 (2010).

[56] Y. Wang, J. Lv, L. Zhu, and Y. Ma, CALYPSO: A method for crystal structure prediction, Comput. Phys. Commun. **183**, 2063 (2012).

[57] Y. Wang, M. Miao, J. Lv, L. Zhu, K. Yin, H. Liu, and Y. Ma, An effective structure prediction method for layered materials based on 2D particle swarm optimization algorithm, J. Chem. Phys. **137**, 224108 (2012).

[58] B. Gao, P. Gao, S. Lu, J. Lv, Y. Wang, and Y. Ma, Interface structure prediction via CALYPSO method, Sci. Bull. **64**, 301 (2019).

[59] X. Shao, J. Lv, P. Liu, S. Shao, P. Gao, H. Liu, Y. Wang, and Y. Ma, A symmetry-orientated divide-and-conquer method for crystal structure prediction, J. Chem. Phys. **156**, 014105 (2022).

[60] W. Kohn and L. J. Sham, Self-consistent equations including exchange and correlation effects, Phys. Rev. **140**, A1133 (1965).

[61] J. P. Perdew, K. Burke, and M. Ernzerhof, Generalized gradient approximation made simple, Phys. Rev. Lett. **77**, 3865 (1996).

[62] G. Kresse and J. Furthmüller, Efficient iterative schemes for *ab initio* total-energy calculations using a plane-wave basis set, Phys. Rev. B **54**, 11169 (1996).

[63] P. E. Blöchl, Projector augmented-wave method, Phys. Rev. B **50**, 17953 (1994).

[64] H. J. Monkhorst and J. D. Pack, Special points for Brillouin-zone integrations, Phys. Rev. B **13**, 5188 (1976).

[65] A. Togo, F. Oba, and I. Tanaka, First-principles calculations of the ferroelastic transition between rutile-type and $CaCl_2$-type SiO_2 at high pressures, Phys. Rev. B **78**, 134106 (2008).

[66] F. Knoop, N. Shulumba, A. Castellano, J. P. Alvarinhas Batistia, R. Farris, M. J. Verstraete, M. Heine, D. Broido, D. S. Kim, J. Klarbring *et al.*, TDEP: Temperature dependent effective potentials, J. Open Source Softw. **9**, 6150 (2024).

[67] O. Hellman, P. Steneteg, I. A. Abrikosov, and S. I. Simak, Temperature dependent effective potential method for accurate free energy calculations of solids, Phys. Rev. B **87**, 104111 (2013).

[68] O. Hellman and I. A. Abrikosov, Temperature-dependent effective third-order interatomic force constants from first principles, Phys. Rev. B **88**, 144301 (2013).

[69] See Supplemental Material at http://link.aps.org/supplemental/10.1103/PhysRevResearch.6.033213. It contains the crystal structures of hybrid compounds, NaN_5ClN_5 and NaN_5BrN_5,

phonon spectra, electronic properties, structural parameters, mulliken population analysis, etc.

[70] W. Zhang, A. R. Oganov, A. F. Goncharov, Q. Zhu, S. E. Boulfelfel, A. O. Lyakhov, E. Stavrou, M. Somayazulu, V. B Prakapenka, and Z. Konôpková, Unexpected stable stoichiometries of sodium chlorides, Science **342**, 1502 (2013).

[71] R. S. Mulliken, Electronic population analysis on LCAO–MO molecular wave functions. I, J. Chem. Phys. **23**, 1833 (1955).

[72] S. Zhang, Q. Yang, X. Liu, X. Qu, Q. Wei, G. Xie, S. Chen, and S. Gao, High-energy metal–organic frameworks (HE-MOFs): Synthesis, structure and energetic performance, Coord. Chem. Rev. **307**, 292 (2016).